Amino Acids (2007) 32: 479–482
DOI 10.1007/s00726-006-0436-5
Printed in The Netherlands

Amino Acids

Crystallization and preliminary X-ray diffraction analysis of *E. coli* arginyl-tRNA synthetase in complex form with a $tRNA^{Arg}$

M. Zhou [1], **A. Azzi** [1], **X. Xia** [2], **E.-D. Wang** [2], and **S.-X. Lin** [1,3]

[1] Laboratory of Molecular Endocrinology, CHUL Research Center and Laval University, Québec, Canada
[2] State Key Laboratory of Molecular Biology, Shanghai Institute of Biochemistry and Cell Biology (SIBCB), Shanghai Institutes of Biological Sciences (SIBS), Shanghai, China
[3] Laboratory for Exchange Visitors and Structural Biology Platform, SIBCB, SIBS, Shanghai, China

Received August 10, 2006
Accepted September 9, 2006
Published online October 24, 2006;

Summary. Amino acids are building blocks of proteins, while aminoacyl-tRNA synthetases (aaRSs) catalyze the first reaction in such building: the biosynthesis of proteins. The *E. coli* arginyl-tRNA synthetase (ArgRS) has been crystallized in complex form with $tRNA^{Arg}$ (*B. stearothermophilus*), at pH 5.6 using ammonium sulfate as a precipitating agent. Two crystal forms have been identified based on unit cell dimension. The complete data sets from both crystal forms have been collected with a primitive hexagonal space group. A data set of Form II crystals at 3.2 Å and 94% completeness has been obtained, with unit cell parameters $a = b = 98.0$ Å, $c = 463.2$ Å, and $\alpha = \beta = 90°$, $\gamma = 120°$, being different from $a = b = 110.8$ Å, $c = 377.8$ Å for form I. The structure determination will demonstrate the interaction of these two macromolecules to understand the special mechanism of ArgRS that requires the presence of tRNA for amino acid activation. Such complex structure also provides a wide opening for inhibitor search using bioinformatics.

Keywords: Amino acids – Arginyl-tRNA synthetase – $tRNA^{Arg}$ – Protein-RNA complex – Macromolecular crystallization – Amino acid activation – Aminoacylation – Protein biosynthesis

Introduction

Aminoacyl-tRNA synthetases (aaRSs) are essential in the first step of protein biosynthesis for catalyzing the aminoacylation of their cognate tRNA molecules. The aaRSs have high specificities toward both tRNAs and amino acids, and there is very limited sequence homology among twenty enzymes specific for different amino acids. According to their conserved sequence in catalytic and characteristic structural motifs, aaRSs can be classified into two classes, each with ten members (Eriani et al., 1990; Ibba and Soll, 2000). Class I enzymes catalyze acylation on the 2′ OH of the ribose of the last adenosine of tRNA, contain a characteristic Rossmann fold and have two conserved signature sequences (HIGH and KMSK) located in the active site. The class II aaRSs are characterized by three homologous motifs, designated as motifs 1, 2, and 3 and aminoacylation occurs on the 3′ OH, except for phenylalanyl-tRNA synthetase (Eriani et al., 1990).

Arginyl-tRNA synthetase (ArgRS) belongs to class I aaRSs. Moreover, it shares a common mechanism with glutamyl-tRNA synthetase (GluRS) and glutaminyl tRNA synthetase (GlnRS), which require the presence of tRNA for the ATP-PPi exchange reaction (Ravel et al., 1964, 1965; Lin et al., 1988a, b). The latter exchange reaction is usually an easy measurement of the amino acid activation for aaRSs. A prolonged scientific debate on their detailed mechanism of aminoacylation since more than 30 years has not provided definite answer to date, but strong evidences that the classical two step reaction were shown by fast kinetic studies (Fersht et al., 1978; Gerlo et al., 1982; Eriani and Cavarelli, 2005). Significant interactions between the substrates via the enzyme template were also demonstrated (Lin et al., 1988b). These three enzymes are classified in the same subclass Ic, and they all use charged or polar amino acids as the substrate. *E. coli* ArgRS however, has the sequence HVGH associated with the Rossmann fold, which is similar to HIGH found in most of the class I aaRSs. Alignment of available ArgRS sequences from different origins revealed that the majority of them lacked the canonical KMSK sequence (Shimada et al., 2001), including those from *Escherichia coli*, *Thermus thermophilus* and *Saccharomyces cerevisiae*. However ArgRS from *Bacillus stearothermophilus* does contain the

KMSK motif (Li et al., 2003). A study on the cross recognition of *E. coli* ArgRS and $tRNA^{Arg}$ from *B. stearothermophilus* showed that at 37 °C the enzyme aminoacylated *B. stearothermophilus* $tRNA^{Arg}$ (ACG) at a similar rate to *E. coli* $tRNA^{Arg}$ (ACG) but with slightly lower tRNA affinity, whereas *B. stearothermophilus* ArgRS did not detectably aminoacylate *E. coli* $tRNA^{Arg}$ (ACG) (Li et al., 2003). *B. stearothermophilus* tRNA was used in this study due to the high homogeneity of its preparation and diffraction quality crystals of its complex with *E. coli* ArgRS.

The 3-D structures of *Saccharomyces cerevisiae* ArgRS/L-arginine binary complex (Cavarelli et al., 1998) and ArgRS/$tRNA^{Arg}$/L-arginine ternary complex (Delagoutte et al., 2000), and the apoenzyme form of *T. thermophilus* ArgRS (Shimada et al., 2001) have been determined. There is 29% sequence identity between *E. coli* and yeast ArgRSs. Here we report the crystallization and preliminary X-ray diffraction analysis of over-expressed *E. coli* ArgRS in complex with *B. stearothermophilus* $tRNA^{Arg}$. The structure resulting from these crystals will provide new information on the interaction between the enzyme protein and the transfer RNA molecule, providing a strong basis for inhibitor design using bioinformatics. In fact, pseudomonic acid, a potent and selective inhibitor of bacterial isoleucyl-tRNA synthetase, is already in clinical use. The combination of crystallography with bioinformatics will eventually accelerate the inhibitor search of the bacterial enzyme (Chou, 2004).

Materials and methods

Materials

Most chemicals were purchased from Sigma-Aldrich Canada (Oakville, Ontario, Canada) including DTT (dithiothretol), EDTA (Ethylene-diamine-tetraacetic acid), PMSF (phenylmethyl sulfonyl fluoride), sodium azide, sodium chloride, sodium phosphates (monobasic and dibasic), and Trizma base. Centricons 30 concentrators were from Millipore (Nepean, Ontario, Canada). Screen kits (I and II) for crystallization were from Hampton Research Inc. (Riverside, California, USA). The media of DEAE Sepharose Fast Flow and Blue Sepharose 6 Fast Flow were bought from Amersham-Biosciences (Baie d'Urfé, Quebec, Canada). The chromatographic columns for protein purification were packed in the laboratory. The gene encoding *B. stearothermophilus* $tRNA^{Arg}$ was cloned, expressed in *E. coli* MT 102, and $tRNA^{Arg}$ was purified as described (Li et al., 2003), $tRNA^{Arg}$ was stored as lyophilized powder, it was resuspended in sterilized H_2O before use and the aliquots can be stored at −20 ° for a short period.

Methods

The gene encoding *E. coli* ArgRS was cloned and the target protein was overproduced and purified according to the previous method (Liu et al., 1999). Briefly, *E. coli* JM109 (DE3) cells containing pMFT7-*argS* were harvested 6 h after induction, 5 grams of wet cells were suspended in 30 ml buffer (containing 40 mM Tris, pH 7.5, 50 mM NaCl, and 20% glycerol) and sonicated. The supernatant from 162,000 × *g* ultracentrifugation was loaded onto a DEAE-Sepharose CL-6B column and eluted with a potassium phosphate gradient. The fractions containing ArgRS were pooled and dialyzed against 10 mM potassium phosphate. We repeated the same chromatography procedure twice to homogeneity >98%, and then purified protein was concentrated to 30–40 mg/ml in the buffer solution containing 10 mM K_2HPO_4∼KH_2PO_4, pH 7.5, and 5% glycerol for crystallization or stored at −20 °C with 50% glycerol. The crystallization was conducted as soon as possible after the purification of enzyme protein.

The *E. coli* ArgRS (MW: 68 kD) and *B. stearothermophilus* $tRNA^{Arg}$ (MW: 25 kD) were mixed at a molar ratio 1:1.2. Crystallization was performed by the hanging-drop vapor diffusion method, starting from matrix-screening kits I and II at room temperature (Jancarik and Kim, 1991; Hampton Research, 1999), and then modified from the initial condition. In the hanging drop, equal volumes of protein/tRNA solution and reservoir solution were used. The protein/tRNA solution contained 0.33 mM ArgRS and 0.4 mM $tRNA^{Arg}$ in the buffer solution indicated above. The reservoir contained 2 M $(NH_4)_2SO_4$ at pH 5.6. To confirm that crystals are formed by ArgRS/tRNA complex molecules, crystals were taken from drop, sequentially washed three times in reservoir solution, then dissolved in water. The OD260/OD280 ratios of the solution from dissolved crystals and that of protein/tRNA (1:1 molar ratio) were checked respectively with Beckman DU-70 spectrophotometer. For cryo-protection during data collection, the crystals were sequentially passed through two drops, both containing a similar concentration of tRNA to that in the hanging drop with a cryo-protectant mixture (of 25% glycerol with 75% well reservoir solution). The addition of the tRNA in the cryo-solution helps to maintain the stability of the crystal. Crystals were then flash-frozen in a liquid nitrogen stream for transportation and data collection at synchrotron. The data collection was carried out at F1 station at CHESS synchrotron at Cornell University and at 14-BM-C in Argonne National Laboratory. Images with oscillations of 0.1° (for crystal form I) and 0.4° (for crystal form II) were collected over 180° range. The exposure time per frame was 15 seconds for form I and 45 seconds for form II. The data were processed with HKL2000 suite (Otwinowski and Minor, 1997).

Results and discussion

The crystals appeared within two to three days after the initiation of the hanging drop, and matured over 5–7 days. They were single, ditrigonal-dipyramid shaped, and reached a size of $0.4 \times 0.4 \times 1.2\,mm^3$ at maturity (Fig. 1). When the ratio of protein sample volume versus that of the reservoir is higher at crystallization initiation (e.g., 1.5:1), it will form hexagonal dipyramid crystals, with a final size of $0.1 \times 0.1 \times 1.5\,mm^3$ (not shown here). Dissolved crystals were first checked on SDS-PAGE with Coomassie blue staining to confirm the protein band (data not shown). They were then checked with OD260/OD280 ratio. OD260/OD280 ratio are 0.6 and 2.1 for purified ArgRS and $tRNA^{Arg}$ respectively, while that reading for dissolved crystals was 1.47, which is comparable with 1.59 (from ArgRS and $tRNA^{Arg}$ solution at 1:1 molar ratio) within experimental error. These spectrophotometer measurements as well as the factor that tRNA is the necessary additive in cryoprotectant convince us that the crystals are in ArgRS/$tRNA^{Arg}$ complex. We have tested several crystals of both forms on synchrotron beamline 14-BM-C at APS at the Argonne National Laboratory and F1 station at Cornell

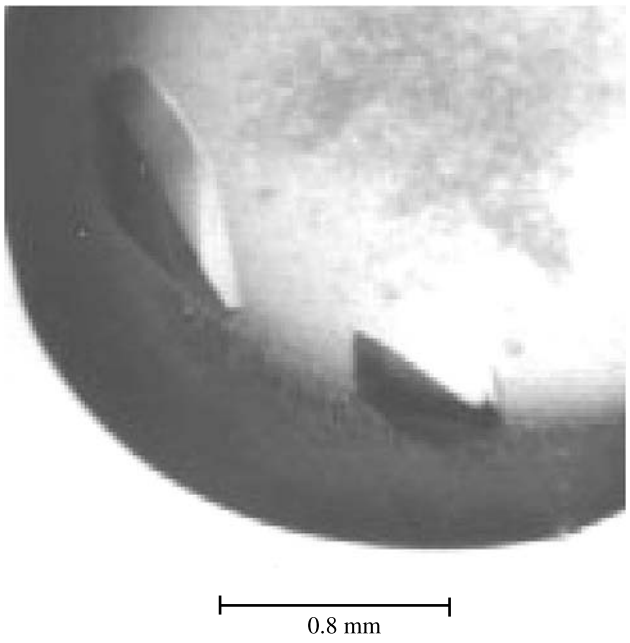

Fig. 1. The ditrigonal-dipyramid shaped crystals of ArgRS/tRNA^{Arg} and their relative size shown below

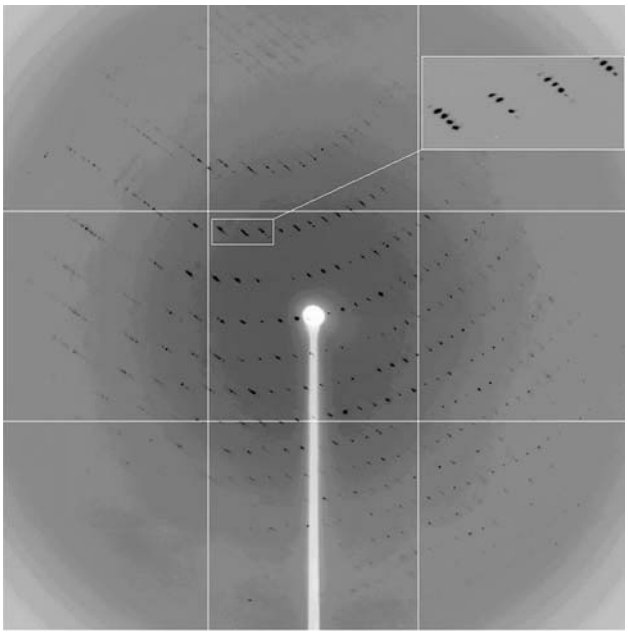

Fig. 2. A representative 0.4° oscillation image from form II ArgRS-tRNA complex. Images were collected at beamline 14 BM-C at Advanced Photon Source on cryo-cooled crystals soaked in 25% glycerol. The inset figure is a magnification of a region to show reflections spots resolution

High Energy Synchrotron Source (CHESS). The data collection parameters were optimized in order to resolve the diffraction maximal. We have identified, from data analysis, two crystal forms with different unit cell parameters as shown in Table 1. Both crystals belong to primitive hexagonal space group P6 and no higher order symmetry was detected based on systematic absences. Crystal form I has unit cell parameters of a = b = 110.8 Å, c = 377.8 Å, and $\alpha = \beta = 90°$, $\gamma = 120°$. Data were processed to 3.5 Å with an Rsym of 8.2% and completeness of 93.1%. Crystal form II has different unit cell parameters: a = b = 98.0 Å, c = 463.2 Å with about 100 Å longer c axis than Form I. We have collected a data set of form II at 3.2 Å (Fig. 2) with completeness of 94% and Rsym of 10%. Several crystals tested have consistently shown that crystal form II diffracted to higher resolution than form I.

Table 1. Data processing statistics

	Form I	Form II
Data collection	CHESS F1	APS Beamline 14-BM-C
Detector	Dual ADSC Quantum-4 CCD	ADSC Quantum-315 CCD
Crystal oscillation (°)	0.1	0.4
Space group	P6	P6
Unit cell lengths (Å)	a = b = 110.8, c = 377.8	a = b = 98.0, c = 463.2
Unit cell volume (Å^3)	83720	90787
Mosaic spread (°)	0.82	0.8
Resolution range (Å)	50–3.5 (3.65–3.5)	50–3.2 (3.32–3.2)
Completeness (%)	93 (95)	94 (97)
Number of measured reflections	2277080	5257759
Number of unique reflections collected	22291	35759
Rsym (%)	8.2 (36.5)	10.1 (39.7)
I/γ	26	8

Value for high resolution shell is between brackets. Rsym = $\Sigma|I_i - \langle I_i\rangle|/\Sigma\langle I_i\rangle$ where I_i is the observed intensity and $\langle I_i\rangle$ is the average intensity over symmetry-equivalent measurement

Attempts to solve the structure with molecular replacement methods using yeast and thermophilus ArgRS were not successful. We have since obtained heavy atom (Pt, Au) derivative crystals to determine the structure by multi-isomorphous replacement.

Meanwhile, we are also working on structural determination of the apoenzyme form of *E. coli* ArgRS on crystals improved from those reported earlier by Zhou et al. (1997). The structural comparison of apo-ArgRS and ArgRS/tRNA^{Arg} complex will help us to better understand the interactions between the enzyme protein and the tRNA molecule, to elucidate the enzyme function and the mechanism of action of the Class Ic aaRSs. It was recently reported that glutamyl-AMP analogs inhibit much more efficiently bacterial GluRS than mammalian GluRSs (Bernier et al., 2005). The combined crystallography with bioinformatics can be very promising in the study of pro-

tein-nucleic acid interactions as well as in the search of selective inhibitors for bacterial ArgRS (Chou, 1994, 2004, 2005; Zhang and Chou, 1994).

Acknowledgements

EDW acknowledges the support to visit Dr. Lin's laboratory at CHUL Research Centre, by the exchange programme between the department of Life Science of the Chinese Natural Science Foundation and "Fonds de Recherche en Sante du Quebec". We also thank the Laboratory of Protein Crystals, Inc., Quebec, Canada for a partial support. We thank Dr. M. Steel and Ms. W. Yang for editing the manuscript.

References

Bernier S, Dubois DY, Habegger-Polomat C, Gagnon LP, Lapointe J, Chenevert R (2005) Glutamylsulfamoyladenosine and pyroglutamyl-sulfamoyladenosine are competitive inhibitors of *E. coli* glutamyl-tRNA synthetase. J Enzym Inhib Med Chem 20: 61–67

Cavarelli J, Delagoutte B, Eriani G, Gangloff J, Moras D (1998) Yeast arginyl-tRNA synthetase with L-Arg. EMBO J 17: 5438–5448

Chou KC (1994) A molecular piston mechanism of pumping protons by bacteriorhodopsin. Amino Acids 7: 1–17

Chou K-C (2004) Structural bioinformatics and its impact to biomedical science. Curr Med Chem 11: 2105–2134

Chou K-C (2005) Insights for modeling in the 3D structure of DNA-CBF3b complex. J Proteome Res 4: 1657–1660

Delagoutte B, Moras D, Cavarelli J (2000) tRNA aminoacylation by arginyl-tRNA synthetase: induced conformations during substrates binding. EMBO J 19: 5599–5610

Eriani G, Delarue M, Poch O, Gangloff J, Moras D (1990) Partition of tRNA synthetase into two classes based on mutually exclusive sets of sequence motif. Nature 347: 203–206

Eriani G, Cavarelli J (2005) Arginyl-tRNA synthetases. In: Ibba M, Francklyn C, Cusack SL (eds) The aminoacyl-tRNA synthetases. Landes bioscience/Eurekah.com, pp 3–11

Fersht A, Gangloff J, Dirheimer G (1978) Reaction pathway and rate-determining step in the aminoacylation of $tRNA^{Arg}$ catalyzed by arginyl-tRNA synthetase from yeast. Biochemistry 17: 3740–3746

Gerlo E, Freist W, Charlier J (1982) Arginyl-tRNA synthetases from Escherichia coli K12: Specificity with regard to ATP analogs and their magnesium complexes. Hoppe Seylers Z Physiol Chem 363: 365–373

Hampton Research (1999) Crystallization research tools 9, p 4

Ibba M, Soll D (2000) Aminoacyl-tRNA synthesis. Annu Rev Biochem 69: 617–650

Jancarik J, Kim SH (1991) Sparse matrix sampling a screening method for crystallization of proteins. J Appl Cryst 24: 409–411

Li J, Yao Y-N, Liu M-F, Wang ED (2003) Arginyl-tRNA synthetase with signature sequence KMSK from *Bacillus stearothermophilus*. Biochem J 376: 773–779

Lin S-X, Shi JP, Cheng XD, Wang Y-L (1988a) Arginyl-tRNA synthetase from *Escherichia coli*, purification by affinity chromatogaphy, properties, and steady-state kinetics. Biochemistry 27: 6343–6348

Lin S-X, Wang Q, Wang Y-L (1988b) Interaction between *Escherichia coli* arginyl-tRNA synthetase and its substrates. Biochemistry 27: 6348–6353

Liu W, Wang E-D, Wang Y-L (1999) A novel system for hyper expression and rapid purification of arginyl-tRNA synthetase from *Escherichia coli*. Acta Biochim Biophys Sinica 31: 494–498

Otwinowski Z, Minor W (1997) Processing of X-ray diffraction data collected in oscillation mode. In: Carter CW Jr, Sweet RM (eds) Macromolecular crystallography. Part A. Methods in enzymology, Vol. 276. Academic Press, New York, pp 307–326

Ravel J, Wang SF, Shive W (1964) Separation and properties of the glutamyl- and glutaminyl-tRNA synthetases of *E. coli W*. Fed Proc 23: 381

Ravel J, Wang S, Heinemeyer C, Shive W (1965) Glutamyl and glutaminyl ribonucleic acid synthetases of *Escherichia coli W*. J Biol Chem 240: 432–438

Shimada A, Nureki S, Goto M, Takahashi S, Yokoyama S (2001) Structural and mutational studies of the recognition of the arginine tRNA-specific major identity element, A20, by arginyl-tRNA synthetase. Proc Natl Acad Sci USA 98: 13537–13542

Zhang C-T, Chou K-C (1994) A graphic approach to analyzing codon usage in 1562 *Escherichia coli* protein coding sequences. J Mol Biol 238: 1–8

Zhou M, Wang E-D, Campbell RL, Wang Y-L, Lin S-X (1997) Crystallization and preliminary X-ray diffraction analysis of arginyl-tRNA synthetase from *Escherichia coli*. Protein Sci 6: 2636–2638

Authors' address: Sheng-Xiang Lin, CHUL Research Center, 2705 Boulevard Laurier, Québec G1V 4G2, Canada,
Fax: +1-418-654-2761, E-mail: sxlin@crchul.ulaval.ca